Atmos. Meas. Tech. Discuss., 6, 10889–10920, 2013
www.atmos-meas-tech-discuss.net/6/10889/2013/
doi:10.5194/amtd-6-10889-2013

Atmospheric Measurement Techniques
Discussions
Open Access

Introduction to the in orbit test and its performance of the first meteorological imager of the Communication, Ocean, and Meteorological Satellite

D. Kim[1] **and M. H. Ahn**[2]

[1]National Meteorological Satellite Center/KMA, 636-10 Gwanghyewon-Li, Jincheon-gun, Chungcheongbuk-do, Republic of Korea
[2]Department of Atmospheric Science and Engineering, Ewha Womans University, Ewha-Yeodae-Gil 52, Seodaemoon-Gu, Seoul, Republic of Korea

Received: 13 August 2013 – Accepted: 2 December 2013 – Published: 17 December 2013

Correspondence to: M. H. Ahn (terryahn65@ewha.ac.kr)

Published by Copernicus Publications on behalf of the European Geosciences Union.

Abstract

The first geostationary earth observation satellite of Korea, named Communication, Ocean, and Meteorological Satellite (COMS), is successfully launched on 27 June 2010 in Korea Standard Time. After arrival of its operational orbit, the satellite underwent in orbit test (IOT) lasting for about 8 months. During the IOT period, the meteorological imager went through tests for its functional and performance demonstration. With the successful acquisition of the first visible channel image, signal chain from the payload to satellite bus and to the ground is also verified. While waiting for the outgassing operation, several functional tests for the payload are also performed. By taking an observation of different sizes of image, of various object targets such as the Sun, moon, and internal calibration target, it has been demonstrated that the payload performs as commanded, satisfying its functional requirements. After successful operation of outgassing which lasted about 40 days, the first set of infrared images is also successfully acquired and the full performance test started.

The radiometric performance of the meteorological imager is tested by signal to noise ratio (SNR) for the visible channel, noise equivalent differential temperature (NEdT) for the infrared channels, and pixel to pixel non-uniformity. In case of the visible channel, SNR of all 8 detectors are obtained using the ground measured parameters and background signals obtained in orbit and are larger than 26 at 5 % albedo, exceeding the user requirement value of 10 with a significant margin. The values at 100 % albedo also meet the user requirements. Also, the relative variability of detector responsivity among the 8 visible channels meets the user requirement, showing values of about 10 % of the user requrirement. For the infrared channels, the NEdT of each detector is well within the user requirement and is comparable with or better than the legacy instruments, except the water vapor channel which is slightly noisier than the legacy instruments. The variability of detector responsivity of infrared channels is also below the user requirement, within 40 % of the requirement except shortwave infrared channel. The improved performance result is partly due to the stable and low detector temperature obtained

with the spacecraft design, by installing a single solar panel to the opposite side of the meteorological imager.

1 Introduction

The first multi-purpose geostationary observation satellite of Korea, known as COMS (Communication, Ocean, and Meteorological Satellite), is launched on 27 June 2010 in KST, at Guiana Space Center at Kourou in French Guiana using the Ariane-5 launch vehicle. At 25 min after the launch, the satellite was successfully injected into the transition altitude of 250 km. From that point on, COMS was lifted into the geostationary orbit by using the LAE (Liquid Apogee Engine) of the satellite, and it successfully arrived its service orbit of 128.2° E on 6 July 2010 as planned.

As its name stands for, COMS is designed to perform three major missions, the operational weather observation by using a meteorological imager (MI), oceanography observation with the Geostationary Ocean Color Imager (GOCI), and the space proof of a Ka-band telecommunication payload. These three missions are supported by three different Korean governmental entities such as Korea Meteorological Administration (KMA), Ministry of Oceans and Fisheries (MOF), and finally Korea Communication Commission. The project was developed under the overall responsibility of Korea Aerospace Research Institute (KARI) supported by the Ministry of Science, ICT and Future Planning (MISP). The designed mission lifetime of COMS is 7 yr which is longer than that of usual geostationary meteorological satellite mission, about 5 yr.

Soon after arrival of satellites' service orbit, the in orbit test (IOT) was started and lasted for about 8 months. During the IOT, not only the space component of the program but also the ground facilities are tested, adjusted, demonstrated, and validated. The test is conducted by Astrium EADS who has the overall responsibility of satellite manufacturing with the help from KARI, KMA, KIOST (Korea Institute of Ocean Science and Technology; responsible for the development and operation of the ocean mission), and ETRI (Electronic and Telecommunication Research Institute, who developed

AMTD
6, 10889–10920, 2013

telecommunication payload and will operate the payload). During the test, all of the command and communication activities are conducted at the COMS CDA (Command and Data Acquisition) facility at KARI with the help of the participating organizations. The meteorological data processing facility at National Meteorological Satellite Center (NMSC) of KMA is developed for the backup station of the COMS CDA and primiary station for the real time processing of the MI data. During the IOT, NMSC facility is also used for the backup operation and real time MI data processing.

Here, we introduce the radiometeric characteristics of COMS/MI obtained during the IOT test period, in terms of functional and performance parts. Section 2 introduces the overall specification of COMS/MI, while Sect. 3 shows the functional test results including the first images followed by the characteristics of the radiometeric performance of COMS/MI in Sect. 4. Section 5 summarizes the performance characteristics obtained during the IOT and concludes the paper.

2 COMS/MI

COMS/MI is manufactured by ITT in US which has a long history of meteorological payload production. The predecessors of COMS/MI have long been used for the operational geostationary meteorological mission since the GOES-8 launched in April 1994. COMS/MI is basically an imaging radiometer which has 5 observation channels, one in the visible band (VIS), one in short-wave infrared band (SWIR), one in the water vapor absorption band (WV), and two split window bands (IR1, and IR2). The channel characteristics and specifications of these 5 channels are summarized in Table 1 including the center wavelength, the instantaneous field of view (IFOV) at the sub-satellite position, and dynamic range. The IFOV of 28 µradian and 112 µradian for the visible and infrared channels corresponds to 1 km and 4 km at the geostationary orbit, respectively. The dynamic range for the short-wave infrared is selected to account for the increased input signal by the reflected sun light during the daytime.

AMTD
6, 10889–10920, 2013

To meet the user requirement, COMS/MI is designed with 3 major parts, including electronics, optics, and power supply module. The major functions of electronics module are the command, control, and data processing. The power supply module provides necessary electric power for electronics and sensor module by interfacing with the spacecraft. The sensor module is the main component for the actual observation and has the major components including scan assembly, telescope, spectrometer, detectors with the passive cooler, and internal calibration target (a blackbody) and albedo monitor. COMS/MI uses a Cassegrain type telescope with the primary and secondary reflecting mirrors having a diameter of 31.1 cm and 3.8 cm, respectively. The two-axis gimbaled scanner sweeps E–W direction with 8 km width (N–S direction) in $20.0^{\circ}\,s^{-1}$ optical speed. This results in the scanning time of about 27 min to cover the full disk of earth which covers about 17.7° of field of regard for NS and EW directions.

The incident radiation coming through the telescope is separated by the series of beam splitters before entering into the detectors. The first Dichroic beam splitter reflects infrared radiation into the next infrared Dichroic beam splitter, while it transmits visible radiation into the 8 visible detectors (corresponding 1 km spatial resolution) which are operated under the ambient temperature. The infrared radiation undergoes further separation into the specified band wavelengths through the series of the beam splitter and band pass filters. There are two detectors for each channel (corresponding 4 km spatial resolution) which are mounted on the same patch. The operational temperature required for the IR detectors are cryogenic temperature and are obtained by a passive radiant cooler which has three stages of the vacuum housing, the radiator, and the patch. To achieve the maximum performance of the passive cooler, the spacecraft is designed to minimize interference of the cooler by securing full field of regard of vacuum housing and incident of external light into the cooler.

For the radiometeric calibration, COMS/MI has two components, a blackbody for the infrared channels and albedo monitor for the visible channel. The blackbody is installed on the baseplate of the sensor module, while the albedo monitor is located underneath of the sensor module. As the blackbody is used for the warm target, its temperature needs to be regulated at a fixed temperature with a certain range of variability. This is done by using the heat pipes which regulate the blackbody temperature within the specification. For a better temperature reading of the blackbody, there are 8 thermistors embedded under the blackbody surface. Another target for the infrared channel calibration, the cold target, is provided by the space which has fairly stable background temperature of about 2.7 K. Thus for the infrared calibration, the scan mirror needs to look at the blackbody and space.

On the other hand, there is no true on-board calibration target for the visible channel. Thus, an absolute calibration of the visible channel needs to resort to other methods such as the vicarious calibrations using reference target method (Wu et al., 2011; Chun et al., 2012) or satellite to satellite intercomparision (Chander et al., 2013). However, there is one component, the albedo monitor, which can be used for the monitoring of an overall trend of telescope mirrors (excluding the scan mirror) and spectrometer characteristics. It reflects solar radiation into the optical chain (to the primary mirror) when the satellite is in right alignment with the Sun (it usually occurs early in the satellite morning hour). As the reflected solar radiation from the albedo monitor shine only small portion of the primary mirror and secondary mirror, the signal is only detected by a specific detector among the 8 detectors (see Fig. 4). Due to the partial exposure of the optical chain to solar radiation, the measured data are only used for the monitoring of an overall trend, not for an absolute calibration of the visible channels.

One of the most important overall sensor characteristics is the spectral response function (SRF) which represents the weights applied to the input signal to detector output. SRF for the infrared channels for the two different sides of detector sets are obtained before the launch of satellite. Figure 1 shows the comparison of spectral response functions of COMS/MI and other legacy instruments, such as MTSAT-2, GOES-13 and -15. Although the band center and width are quite similar, there are differences. For example, bandwidth of the water vapor channel for COMS/MI is much narrower than for GOES series. In case of the SWIR channel, the center wavelelgth of COMS/MI is slightly shorter than GOES series, with the expectation of less contamination by

AMTD
6, 10889–10920, 2013

the CO_2 absorption. The COMS/MI SRFs are available at the KMA/NMSC webpage (http://nmsc.kma.go.kr/html/homepage/ko/information/News/searchNews.do).

3 In orbit test

Soon after the arrival of its service orbit, the IOT was started. The major goals for the IOT are to make sure that COMS and its payloads have survived the launch campaign, to demonstrate that the performances at space are in line with the predicted performance, and to collect information and data for the actual operation of satellite and fine tunings of equipments and algorithms. The IOT activities could be categorized into a system and payload, functional and performance, and preparation of operation. The original plan for the IOT was about 6 months, although the actual period was about 8 months which is considered quite a successful compared to the other similar programs.

During the IOT, COMS/MI also underwent a series of tests and performance evaluations. To meet the purposes of the COMS/MI IOT test, its activity includes the verification of the command and control of the MI, such as the command execution, mode switching, redundancy selection of the MI channels and monitoring of the instrument through the direct telemetry. It also includes the verification of radiometric performances, such as visible and infrared channel radiometry, visible channel response verification using albedo monitor, and verification of the continued image acquisition throughout the earth eclipse time period. It also includes the fine tuning of the image navigation and registration (INR) algorithms and its extensive verification of performances at system level, i.e. INR validation, band to band registration, navigation performance. For COMS/MI, there are several important IOT stages to be mentioned here, which depended on the operational phases of IOT.

3.1 Launch and orbit raising

During this phase, MI is in stand-by mode and the MI housekeeping telemetry data is available via the satellite for the health check and monitoring of COMS/MI. Because COMS/MI does not have any protective cover to prevent direct solar intrusion into the primary mirror of instrument, a careful plan to prevent direct looking of sun was prepared and exercised. Other than that, IOT activity during this phase is limited to housekeeping telemetry monitoring.

3.2 Outgassing operation

The coldest parts of MI such as the infrared detectors are susceptible for the contamination. To minimize the contamination to the sensitive part of the instrument, special cares are applied. For example, during the launch and orbit raising period, the cold part is covered by the cooler cover. Also, as soon as possible, the outgassing mode is switched on to heat up the infrared detector suite and passive cooler to bake out any contaminants from the surface of these parts. In the case of the COMS IOT, it lasted about six weeks (same as the typically recommended 42 days) from launch date to 11 August 2010. Even in such a mode, COMS/MI can be operated, although there is no valid data from the IR channels: the visible channel imagery and scan mechanism are fully operational since 12 July 2010 when the first visible images are taken.

3.3 Full tests

As soon as the outgassing period ends, the COMS/MI radiant cooler is deployed into the operation mode (i.e. opened the passive-cooler cover and the cover is attached to a side of COMS/MI). With the opening of cooler cover, the COMS/MI radiant cooler cools down the detector patch to a stabilized, regulated patch temperature. It takes about one day to finish the cooling and stabilization processes and the acquisition of the infrared images is started. The acquisition of the first four infrared images from the

AMTD
6, 10889–10920, 2013

COMS/MI is also finished without any significant issue. After the successful start of full operation of the COMS/MI, the IOT is resumed for the all five channels.

4 Results

Performance results are described in the functional and radiometric perspective. In actual orbit tests, functional test was conducted first followed by the performance test.

4.1 Functional performance

The first COMS/MI image was taken soon after the successful arrival of service orbit, from 02:15 UTC to 02:45 UTC, on 12 July 2010. Figure 2 shows the original and rectified images of the visible channel. The original image, which is not underwent any image navigation nor radiometric calibration, is oversampled by a factor of 1.75, while the rectified image is obtained by re-sampling of the original image. At the center of the image, the second tropical cyclone of the year, Conson, is clearly captured, with the bright circle of the sun glint which happen to be in the southeast of the typhoon. Also, another important meteorological feature, the Asia monsoon, is clearly visible with the EW cloud bands which extend from southern China, through Korea, and to over Japan. Successful acquisition and the process of the first image proves the integrity of the whole signal flow, from the radiance measurement by COMS/MI, through the onboard signal processing and transmission, to the reception and processing of signals at the ground station.

After the successful acquisition of the first visible images, several functional tests were conducted for the visible channel and the instrument itself. For example, image acquisition time and scan rate are tested and verified. When COMS/MI is first commanded to take images of 19.48° EW and 17.75° NS (viewing angles at the geostationary orbit), it takes slightly more than 27 min (which is the user's requirement), by about 3 s. Thus the EW scan width is reduced to 19.27° which results in the reduction of the acquisition time to 26 min and 48 s satisfying the user's requirement. Another functional test was to test the scan mechanism and coordination accuracy. In order to do that, a series of moon images are acquired with the anticipation of visible channel calibration (Grant et al., 2001; Wu et al., 2006), of which the moon images could be used as the baseline for further long-term monitoring of the sensor degradation. Figure 3 shows the first series of lunar image taken in 28 July, 16 days after the start of visible channel observation. The series of images clearly indicate the accuracy of coordiante system and a proper functioning of the scan mechanism and its stability. Finally, a test for the model of the orientation of satellite, sun, the earth and scan mechanism is conducted by taking the Sun image through the albedo monitor. Figure 4 shows the sequence images of the Sun taken at one of the visible channels during the test.

After the successful outgassing operation, the first infrared images were taken in 11 August and the first images of four infrared channels are shown in Fig. 5. From the two window channels (Fig. 5a and b), several prominent cloud patterns associated with important weather processes such as the tropical convective activities (center of image), weakened Asia monsoon (upper part of the image), and well developed polar cyclone in the Southern Hemisphere are clearly captured. The water vapor image (Fig. 5d) reveals the well correlated upper air flow associated with those prominent cloud patterns. And finally the short wave infrared image shows its characteristic features of strong temperature sensitivity (for example, upper left part of the image is much darker (i.e. warmer) than other part of image due to the effect of weak solar radiation). Overall, the first trial to acquire all five channel images was quite a success.

With the successful acquisition of all 5 channel images, further functional and performance tests were conducted. One of the most important additional functional tests was the accuracy of image navigation and registration algorithm which determines not only quality of images but also the accuracy of the derived products which use the consecutive images such as the atmospheric motion vector which uses three consecutive images, daily or weekly sea surface temperature which composite all available images for the given time period. With several adjustments of pre-launch algorithm and

AMTD
6, 10889–10920, 2013

refinement of key algorithm parameters through the utilization of actual observation data, the achieved INR performance is quite a success, the INR accuracy is smaller than 1 infrared image pixel (Astrium EADS 2011b). The success is partly due to the successful stabilization of the spacecraft itself (a detailed description of the processes and results are under preparation) and the maximum utilization of avaliable landmarks within the fied of regards of COMS/MI (Astrium EADS 2011b).

One of the important improvements with COMS/MI over the legacy spacecraft and instrument was the expectation of continuous operation during the eclipse period and resilience to the direct solar intrusion to the optical cavity. With this improvement, COMS/MI could provide a continuous observation capability throughout the satellite midnight and a quite stable acquisition of image. The demonstartion test for this capability was conducted on 20 August 2010 and the results are shown in Fig. 6. As the Sun is the opposite side of the satellite-faced earth's surface, the visible channel image shows dark earth disk with the bright sun shining at the top of the image. During this time of day, the visible channel does not provide any meaningful information and thus the solar intrusion does not carry a significant meaning to the operational use of data. On the other hand, as the 4 infrared images provide meaningful information, it is important to minimize or characterize the solar intrusion. As shown in Fig. 6, all four infrared images carry the meaningfull information, although there is affected area by the solar intrusion. The effect is shown to be enhanced at the shortwave infrared channel image, because of the radiance sensitivity of the channel, with the decreasing of the effect with the increasing wavelength, toward the 12 micrometer window channels. From the results, we could verify that the operation interruption due to the so-called keep out zone could be minimized.

4.2 Radiometeric performance

The test results for the radiometric performance demonstrates that COMS/MI satisfies the end user requirements with a significant margin for most of cases. Here, we show the performance results of COMS/MI in terms of noise performance and detector to

AMTD
6, 10889–10920, 2013

detector variation for both the visible and infrared channels. The noise performance is presented as the signal to noise ratio (SNR) for the visible channel and noise equivalent differential temperature (NEdT) for the infrared channels. Pixel-to-pixel Response Nonuniformity (PRNU) provides the degree of differential responsivity for different detectors. The noise and PRNU are evaluated from the space look data which is obtained by looking at the space scene away from the earth scene with the calibration parameters obtained during the ground test of instrument. This space look happens when COMS/MI takes either a full disk observation or by sending a specific command.

To make sure that the selected IFOVs for the performance tests are free from the interference by earth, moon, or sun, the space look scene is carefully selected. This is also important for the infrared channel calibration, because the space look data are used for the background bias correction which should be applied before derivation of the calibration coefficients (Weinreb et al., 1997). To have stable statistical outputs and to minimize any unexpected interference, sensitivity of the background count values as a function of selected IFOV number and location is analyzed. Figure 7 shows an example of such a sensitivity test, which shows the mean and standard deviation of a detector count value of 8 different visible detectors with the different number of IFOVs selected to calculate the mean and standard deviation. Also, we found that the background count value is quite stable from about 100 IFOVs away from the edge of image. Based on these test results, we choose 100 by 100 IFOVs selected from 100 IFOVs away from the upper and left or right edge of the image.

4.2.1 Visible channel

The SNR requirement for the visible channel of COMS/MI is at 5 % and 100 %, in view of quantative use of the visible radiances taken over refecting surfaces having low reflectivity. This is specifically important for the quantative derivation of aerosol optical depth such as the Asian dust using the single channel data (Kim et al., 2007). The SNR at 5 % albedo is estimated by using the Eq. (1) (Astrium EADS, 2011a),

$$\mathrm{SNR}_{5\,\%} = \frac{R_{5\,\%}}{\sqrt{A_{\mathrm{in\_orbit}} + B_{\mathrm{on\_ground}} \times R_{5\,\%}}} \tag{1}$$

where $R_{5\,\%}$ is the radiance at 5 % albedo, $A_{\mathrm{in\_orbit}}$ is the square of the noise radiance obtained from the space look, and $B_{\mathrm{on\_ground}}$ is the correction coefficient obtained from the ground tests conducted before the launch and estimated to be about 0.0021 (in unit of radiance). The calculated $R_{5\,\%}$ varies mainly with the spectral response function of the specific channels and the applied value for the COMS visible channels is estimated to be 23.92 $\mathrm{W\,m^{-2}\,sr^{-1}\,\mu m^{-1}}$. Thus the in orbit SNR value is mainly determined by $A_{\mathrm{in\_orbit}}$ which in turn obtained by the relationship of $A_{\mathrm{in\_orbit}} = (m \times \sigma_{\mathrm{c}})^2$ where the m is the slope for conversion from count value to radiance of each visible detector and σ_{c} is the standard deviation of dark count values obtained from the space look counts. The slope is obtained during the ground test and differs for each detector. For example, m value for the detector number one is about 0.594, while it is about 0.632 for the detector number 5 (Astrium EADS, 2011a).

Table 2 summarizes the SNR values of the 8 visible detectors at 5 % albedo. The mean background count values obtained in orbit are almost the same (maximum difference is less than 0.8 counts) as the values derived at the ground. The standard deviation of 100 by 100 IFOVs is the key parameter that determines the SNR value and shows a quite small number, smaller than 1.5. In consequence, the derived SNR value is larger than 26 for all 8 detectors. These performance results of COMS/MI are well within the user requirement (better than 10) and are also comparable with the legacy instruments (Hillger and Schmidt, 2011).

The image quality, especially for the imaging instrument such as COMS/MI, is also dependent on the relative channel characteristics among the 8 detectors. For example, even though all 8 detectors meet the quality requirements such as SNR, if relative performances are too different among the 8 detectors, the overall image quality will be degraded. To detect the relative performance and mitigate the severe difference if there is any, the detector uniformity is estimated using the pixel to pixel response nonuniformity values. The PRNU values for the COMS/MI visible channels are obtained from the difference between the detectors at 5 % albedo using Eq. (2)

$$\mathrm{PRNU} = \frac{1}{N_{5\,\%}} \sum_{N_{5\,\%}} (R_{\mathrm{Det\_R}} - R_{\mathrm{Det\_i}}) \leq \frac{R_{5\,\%}}{3 \times \mathrm{SNR}_{5\,\%}} \tag{2}$$

where $N_{5\,\%}$ denotes number of space look count used for the calculation, while $R_{\mathrm{Det\_R}}$ and $R_{\mathrm{Det\_i}}$ are the radiance values at the reference detector and the individual dector, respectively. Here, we use the detector number 1 as our reference detector. As shown above equation, the user requirement of the PRNU value is less than 1/3 of noise equivalent delta radiance (NEdR) which is derived from SNR at 5 % albedo.

The overall PRNU performance of the side 1 and side 2 of the visible channel detectors, side 1 is the operational and side 2 is backup, are shown in Table 3. The performance values are obtained from the full disk images taken during the 24 h of operation on 10 to 11 August and on 15 August for side 1 and side 2, respectively. The PRNU values at 7 other detectors are all well below the requirement ($0.8\,\mathrm{W\,m^{-2}\,sr^{-1}\,\mu m^{-1}}$) with a significant margin. The quantative results also confirmed by the qualitative inspection of the visible channels obtained during the test period. However, the PRNU values during around local midnight are larger than the requirement, although this does not carry a significant meaning. The visible channel data obtained during this time of day are not used. Second, the PRNU values is derived before any correction of the stray light or direct sun intrusion effects which significantly degrade the radiometeric performances. The overall results concluded that there is no need of any additional processing such as the normalization of detector signals on the visible channels.

4.2.2 Infared channels

The radiometeric perfomance of the infrared channels depends on many parameters such as the scan mirror emissivity, detector patch temperature in terms of absolute

AMTD
6, 10889–10920, 2013

value and stability, accurate knowledge of the internal calibration target, control of the stray light, overall instrument alighmnent, etc. The overall performance parameters such as NedT and PRNU are the results of combined effects of all these parameters. Thus, here we introduce several activities to improve the overall performance and briefly summurize the IOT results.

For the infrared channels, one of the most well known external source of uncertainty is the scan angle dependence of scan mirror emissivity (Weinreb et al., 1997; MacDonald, 1999). To mitigate this effect, a new coating material for the scan mirror is applied for COMS/MI and the performance is evaluated using the space look count (Astrium EADS, 2011a), which is obtained by scanning full width of EW direction for the area well above the earth disk edge. By using the space look count, a quadratic correction coefficients for the scan angle dependence are derived (Astrium EADS, 2011c). To check the stability of the correction coefficients, the dependence is checked for a short time period, during the 24 h of a day, and for a longer time period, separated about two months, first one in 16 August and second one in 11 October. Based on the test results (Astirum EADS, 2011a), we found that the effect of the scan mirror emissivity does not depend on the detector temperature, there is no significant scan angle dependence in the shortwave infrared channel, and there is no significant temporal variation in the scan angle correction parameters. We thus conclude that the emissivity correction as a function of scan angle is necessary for the infrared channels except the SWIR channel and the fixed correction coefficients are applicable for a short and longer term, although it is recommended for a regular monitoring for a longer term drift.

Another well known calibration uncertainty arises during the satellite midnight when the direct solar radiation can impinge on the internal blackbody. When this happens, the direct radiatation interferes the regulation of the blackbody temperature at a constant temperature and introduces error in the measured blackbody radiation through the reflection of the incident light by the imperfect blackbody. Thus, the overall calibration uncertainty increases and a corrective measure should be applied (Johnson and Weinreb, 1996). To correct this effect, a sensitivity test for the dependence of the

AMTD
6, 10889–10920, 2013

D. Kim and M. H. Ahn

calibration slope to the different sets of temperatures of optics componets such as the scan mirror, primary and secondary mirror, louvre, has been conducted. From the sensitivity tests, the closest correction parameter is obtained from the temperature of scan mirror for the SWIR channel and of the primary mirror for the other infrared channels. Thus, combining the day time calibration slope and night time slope with the the temperature information for the previous 5 days, the midnight calibration correction is succssfully applied (Astrium EADS, 2011a).

After applications of developed measures for the all identified uncertainty sources, the noise performances are derived. Table 4 shows the resultant NEdT values of the four infrared channels of COMS/MI at 220 K and 300 K, and corresponding user requirment specifications. For the estimation of the NEdT values, following procedure is applied.

$$\mathrm{NEdT} = (A + B \times T) - T_{\mathrm{ref}} \tag{3}$$

And T is obtained by conversion of the Planck function,

$$T = \frac{10^6 hc}{\ln\left(\frac{2.\times 10^{24} hc^2}{\lambda_c^5 R}\right)\lambda_c k} \tag{4}$$

where h is the Planck constant (6.62617×10^{-34} J s), c is the speed of light at vacuum (2.99792458×10^{8} m s^{-1}), k is the Boltzmann constant (1.38066×10^{-23} J K^{-1}), and the λ_c is the central wavelength of the infrared channels. A, and B are the conversion coefficient between effective and brightness temperature. Reference temperature T_{ref} is 220 K for space look count and 300 K for the blackbody radiance. The performance values given in Table 4 clearly shows that the noise values of each detector and channel are less than the specification and meet the user's requirement with a significant margin, especially at 220 K. All 8 detectors show that the NEdT values at 220 K are better than the requirement by more than two folds. Even at 300 K, there is a significant

AMTD
6, 10889–10920, 2013

margin at the IR1 and IR2 channels, although the SWIR and WV channels have a less margin.

When these NEdT values given in Table 4 are compared with those of the legacy instruments as shown in Table 5, the noise performance of COMS/MI is comparable or slightly worse than the most current GOES series (i.e. GOES-13, -14, and -15) which utilize the single solar panel spacecraft configuration similar to the COMS configuration. On the other hand, the noise performances of COMS/MI is better than those of legacy instruments onboard the previous GOES series which uses a single solar panel and a balance boom at the opposite side of spacecraft where the imager is located (SS/Loral, 1996). The reflected solar radiation by the balance boom adds a heat source to the imager and the regulated patch temperature was 94 K (during the winter solstice and was 101 K for the other 6 months). However, in case of COMS/MI, the operational patch temperature is 85 K due to the spacecraft design of the single solar panel located at the opposite side of MI instrument.

Although there is only two different detectors for each infrared channel (compared to the 8 detectors for the visible channels), the PRNU for each infrared channels are estimated. The obtained values at 220 K and 300 K are all within the specification (not shown). The ratios of the measured PRNU to PRNU requirement (i.e. 0.0007 for SWIR, 0.007 for WV, and 0.005 and 0.008 for IR1 and IR2, respectively) are within about 30 % except SWIR whose values reach up to 80 % of the requirement at 300 K. From these performance results, we conclude that the IOT test results for the operational infrared channels are within the user requirement and the COMS/MI was commissioned on 1 April 2011, just 9 month after launch of the satellite.

5 Summary

The first geostationary earth observation satellite of Korea, COMS, is launched on 27 June 2010. Soon after the arrival of the satellite in the operational orbit of 128.2° E, in orbit test (IOT) is started that lasted to about 8 months. The tests for the operational use

AMTD
6, 10889–10920, 2013

of the meteorological imager, COMS/MI, started with the acquisition of the first visible channel images on 12 July 2010. With the successful test for acquisition, processing, and dissemination of the data, the overall signal processing chains are verified. During the outgassing period, functional tests of COMS/MI such as the command execution, mode switching, redundancy selection of the MI channels, coordinate verification, scan time are conducted without any significant problem. During the tests, several interesting images such as the series of moon and albedo monitor are also acquired.

After successful acquisition of the four infrared channels, a full functional and performance test are started. It also includes the fine tuning of the image navigation and registration algorithms and its extensive verification of performances at system level. All of the functional and performance estimations obtained during the IOT are all within the specifications and meet requirement for the operational applications. The noise values are all comparable with the most recent series of legacy instruments and better than the previous legacy instruments. More importantly, the designed performances are achieved within 8 months after the launch of satellite (original plan was 6 months). With the succefull performance of IOT, it is concluded that COMS and its payloads are ready to full service and its service started from 1 April 2011.

The data acquired during the in orbit test will play an important role in understanding the nature and characteristics of the current and future COMS/MI data. Thus it is highly recommended to process with the all the updated parameters and make it available to the users. It would be quite important to make these valuable data to as many as users for the further utilization of the COMS/MI data. New and innovative perspectives on the first set of observed data would generate a new and better way for the characterization of a new instrument planned for the next generation of COMS.

Acknowledgements. The authors are indebted to the people worked hard during the in orbit test. It is hard to name each person from Astrium of EADS, KARI, and NMSC. Without their devotion and expertise, the successful results of IOT would not be possible or would be delayed much longer than actually spent. D. Kim is supported by the National Meteorological

Satellite Center (Project No. 153-3100-3137-302-210-13). M. H. Ahn is partially supported by the Ewha Womans University Research Grant of 2012 and by the Eco Innovation Program of KEITI (2012000160002).

References

Astrium EADS: COMS Meteo-Imager In-Orbit Test Report, including Image Quality Verification Report, COMS.RP.00345.DP.T.ASTR, 169 pp., 2011a.

Astrium EADS: COMS INR In-Orbit Test Report, including Image Quality Verification Report, COMS.RP.00347.DP.T.ASTR, 52 pp., 2011b.

Astrium EADS: Meteo-Imager Radiometric Model, COMS.TN.00116.DP.T.ASTR, 133 pp., 2011c.

Chander, G., Hewison, T. J., Fox, N., Wu, X., Xiong, X., and Blackwell, W. J.: Overview of intercalibration of satellite instruments, IEEE T. Geosci. Remote, 51, 1056–1080, 2013.

Chun, H.-W., Sohn, B. J., Kim, D.-H., Ahn, M.-H., and Ou, M.-L.: Solar channel calibration using desert targets in Australia: application to the MTSAT-1R, J. Meteol. Soc. Jpn., 90, 191–205, doi:10.2151/jmsj.2012-203, 2012.

Grant, I. F., Kieffer, H. H., Stone, T. C., and Anderson, J. M.: Lunar calibration of the GMS-5 visible band, Proceedings of the International Geophysics and Remote Sensing Symposium 2001, 4, 2769–2771, 2001.

Hillger, D. W. and Schmit, J. J.: The GOES-15 Science Test: Imager and Sounder Radiance and Product Validations, NOAA TR NESDIS 104, 101 pp., Washington DC, 2011.

Johnson, R. X. and Weinreb, M.: GOES-8 Imager midnight effects and slope correction, Proc. SPIE, 2812, 596–607, 1996.

Kim, J., Yoon, J. M., Ahn, M. H., Sohn, B. J., and Lim, H. S.: Retrieving aerosol optical depth using visible and mid-IR channels from geostationary satellite, MTSAT-1R, Int. J. Remote Sens., 29, 6181–6192, 2007.

MacDonald, M. E.: Alternatives to SiO_x for protective scan mirror coatings in remote sensing instruments, Proc. SPIE 3750, Earth Observing Systems IV, 309, doi:10.1117/12.363524, 1999.

SS/Loral: GOES I-M Databook, DRL 101-08, Rev. 1, 186 pp., 1996.

Weinreb, M. P., Jamison, M., Fulton, N., Chen, Y., Johnson, J. X., Bremer, J., Smith, C., and Baucom, J.: Operational calibration of geostationary operational environmental satellite-8 and -9 imagers and sounders, Appl. Optics, 36, 6895–6904, 1997.

Wu, X., Stone, T. C., Yu, F., and Han, D.: Vicarious calibration of GOES Imager visible channel using the Moon, Proc. SPIE, 6296, 2006.

Wu, X., Qian, H., Yu, F., and Beck, T.: Vicarious calibration of GOES visible channel using GOME-2, IGARSS 2011, 1033–1035, 2011.

Table 1. Specifications of the COMS/MI user's requirement. Note that the dynamic range of SWIR goes up to 350 K to accommodate daytime contribution of solar radiation.

Channel	Center Wavelength (µm)	BWHM	Dynamic Range	IFOV(µrad)	GSD (km)	Noise
VIS	0.675	0.55 ~ 080	0–115 %	28	1	SNR> 170 : 1 at 100 % albedo SNR > 10 : 1 at 5 % albedo
SWIR	3.75	3.5 ~ 4.0	4–350 K	112	4	NEdT < 0.10 K rms at 300 K NEdT < 5.7 K rms at 220 K
WV	6.75	6.5 ~ 7.0	4–330 K	112	4	NEdT < 0.12 K rms at 300 K NEdT < 0.85 K rms at 220 K
IR1	10.8	10.3 ~ 11.3	4–330 K	112	4	NEdT < 0.12 K rms at 300 K NEdT < 0.40 K rms at 220 K
IR2	12.0	11.5 ~ 12.5	4–330 K	112	4	NEdT < 0.20 K rms at 300 K NEdT < 0.48 K rms at 220 K

VIS: Visible
SWIR: Short-Wave InfraRed
WV: Water Vapor
WIN1: Window 1
WIN2: Window 2
BWMH: Band Width at Half Maximum
GSD: Ground Sampling Distance in unit of km

AMTD
6, 10889–10920, 2013

Table 2. The mean and standard deviation (σ) of space look count and the derived signal to noise ratio (SNR) at 5 % and 100 % albedo (reference band radiances for albedo of 5 % is 23.92 $\mathrm{W\,m^{-2}\,sr^{-1}\,\mu m^{-1}}$). The user requirement for SNR of 10 is given at 5 % albedo.

Detector	Mean(Orbit)	σ	Mean (Ground)	SNR (at 5 % albedo)
1	46.48	1.39	47	27.18
2	41.25	1.43	42	26.28
3	40.53	1.44	41	26.20
4	41.71	1.41	42	27.01
5	45.65	1.50	46	25.24
6	39.61	1.39	40	27.08
7	39.52	1.44	40	26.00
8	36.84	1.43	37	26.21

AMTD
6, 10889–10920, 2013

Table 3. PRNU of VIS detectors at 5 ± 1 % albedo. PRNU should be less than 1/3 of noise equivalent delta radiance derived from SNR at 5 % albedo ($0.8\,\mathrm{W\,m^{-2}\,sr^{-1}\,\mu m^{-1}}$).

Detector	PRNU at 5 ± 1 % Albedo (Side 1)	PRNU at 5 ± 1 % Albedo (Side 2)
1	reference	reference
2	0.14	0.06
3	0.13	0.06
4	0.10	0.09
5	0.16	0.02
6	0.02	0.07
7	0.04	0.12
8	0.02	0.17
All detectors	0.09	0.08

AMTD
6, 10889–10920, 2013

Introduction of in orbit test and its performance

D. Kim and M. H. Ahn

Table 4. The noise performance of COMS/MI for each detector with the user required specifications for two different conditions, 220 K and 300 K. The measurement values are given for each detector, although the requirement is the same for the same channel.

Band	Detector	220 K		300 K	
		Measurement	Requirement	Measurement	Requirement
SWIR	A	2.80	5.70	0.07	0.10
	B	2.33		0.07	
WV	A	0.40	0.86	0.08	0.12
	B	0.37		0.06	
IR1	A	0.13	0.40	0.06	0.12
	B	0.14		0.04	
IR2	A	0.23	0.48	0.11	0.20
	B	0.23		0.12	

AMTD
6, 10889–10920, 2013

Table 5. Comparison of COMS/MI noise performance with the legacy instruments onboard previous weather satellite. IR2 channel is not available after GOES-12 which has the new carbon dioxide channel instead of the IR2 channel. The performance values of the legacy instrument are from Hillger and Schmit (2011). In case of COMS/MI, the performance values are for the detector number 1 and number 2.

Band	COMS	G-15	G-14	G-13	G-12	G-11	G-10	G09	G-08
SWIR	0.070 0.070	0.063	0.053	0.051	0.13	0.14	0.17	0.08	0.16
WV	0.080 0.060	0.170	0.18	0.14	0.15	0.22	0.09	0.15	0.27
IR1	0.060 0.040	0.059	0.06	0.053	0.11	0.08	0.20	0.07	0.12
IR2	0.110 0.120					0.20	0.24	0.14	0.20

Discussion Paper | Discussion Paper | Discussion Paper | Discussion Paper |
AMTD
6, 10889–10920, 2013

Introduction of in orbit test and its performance

D. Kim and M. H. Ahn

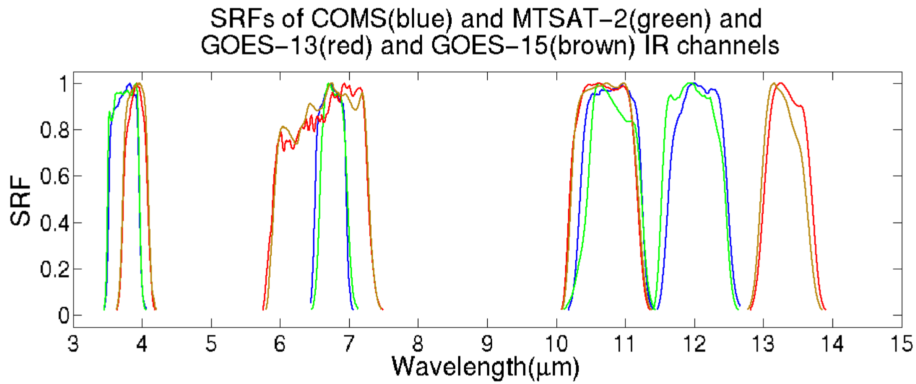

Fig. 1. Comparison of the spectral response function (SRF) of COMS/MI with other legacy instruments onboard GOES-13/-15 and MTSAT-2 satellites.

AMTD
6, 10889–10920, 2013

D. Kim and M. H. Ahn

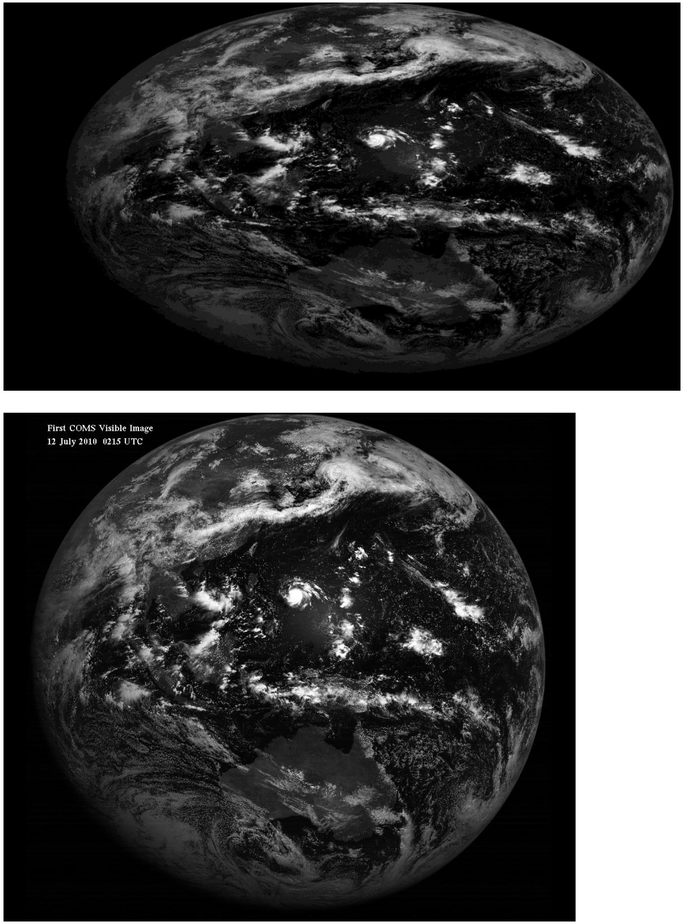

Fig. 2. The first visible images of COMS/MI taken on 12 July 2010. (Top) the original 1.75 oversampled image and (bottom) is the rectified image.

AMTD
6, 10889–10920, 2013

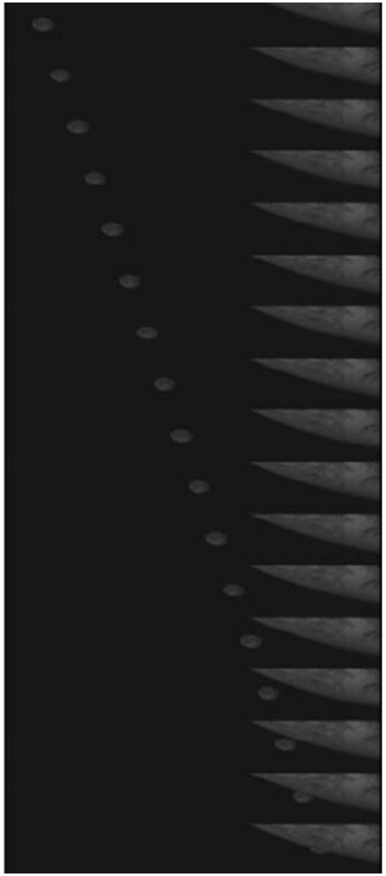

Fig. 3. Series of images taken for the lunar observation on 28 July for the test of the scan mechanism and accuracy of the coordiate system.

AMTD
6, 10889–10920, 2013

Introduction of in orbit test and its performance

D. Kim and M. H. Ahn

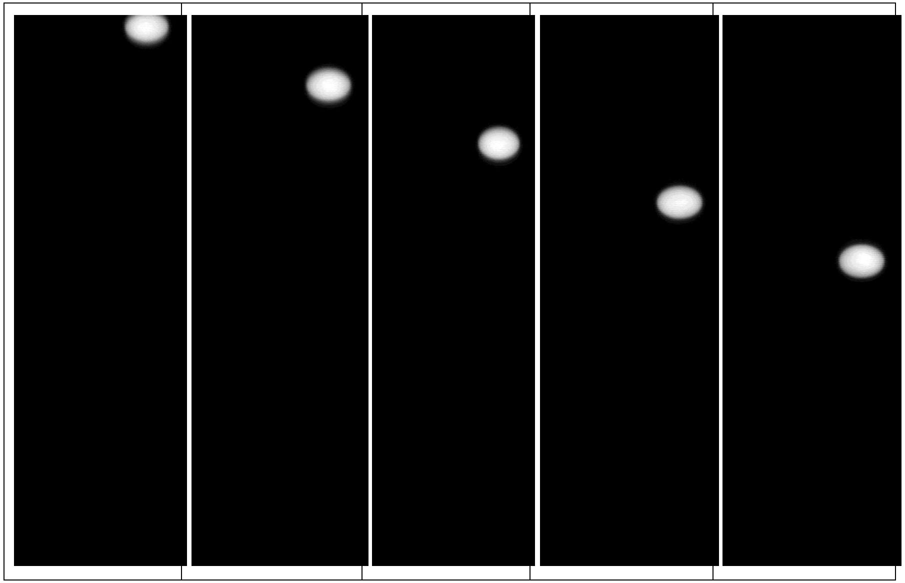

Fig. 4. Sequential images of the Sun captured by one of visible channels through the albedo monitor onboard COMS/MI.

AMTD
6, 10889–10920, 2013

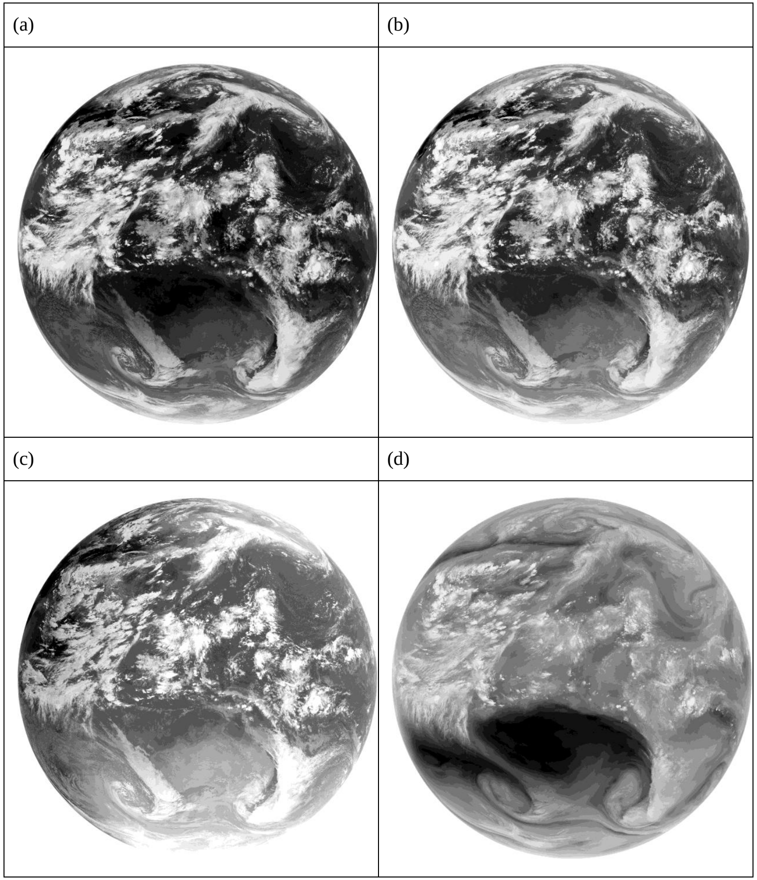

Fig. 5. The first infrared images of COMS/MI taken 12 August 2010. **(a)**, **(b)**, **(c)**, and **(d)** are for IR1, IR2, SWIR, and WV channels, respectivley.

AMTD
6, 10889–10920, 2013

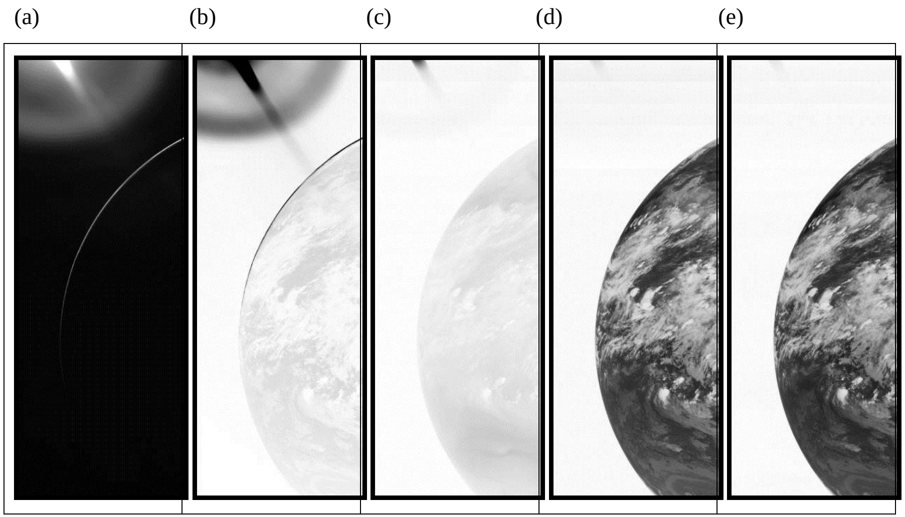

Fig. 6. Effect of solar intrusion to the optical cavity of COMS/MI for different channels **(a)** visible, **(b)** shortwave infrared, **(c)** water vapor, **(d)** and **(e)** are the two infrared window channels on 20 August 2010.

AMTD
6, 10889–10920, 2013

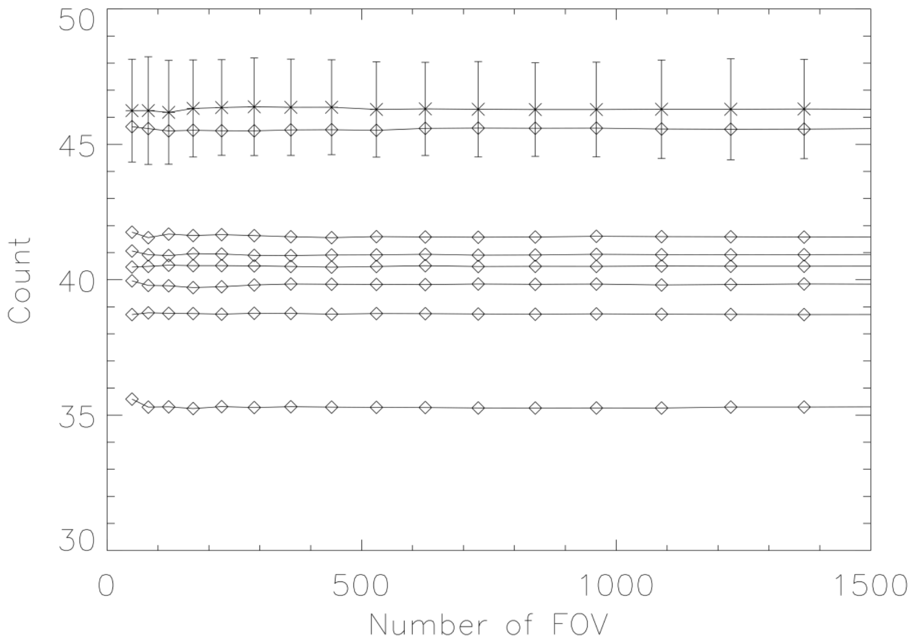

Fig. 7. Variation of average and standard deviation of space-look signal in terms of the digital count value as a function of number of pixels used to estimate the average and standard deviation, given for one detector for clarity (others have a similar magnitude).

AMTD
6, 10889–10920, 2013

Introduction of in orbit test and its performance

D. Kim and M. H. Ahn